This article has been accepted for publication in a future issue of this journal, but has not been fully edited. Content may change prior to final publication. Citation information: DOI 10.1109/TBME.2014.2369991, IEEE Transactions on Biomedical Engineering

Adhesive RFID Sensor Patch for Monitoring of Sweat Electrolytes

Daniel P. Rose, *Graduate Student Member, IEEE*, M. Ratterman, Daniel K. Griffin, Linlin Hou, Nancy Kelley-Loughnane, Rajesh R. Naik, Joshua A. Hagen, I. Papautsky, *Senior Member, IEEE*, and Jason Heikenfeld, *Senior Member, IEEE*

***Abstract*— Wearable digital health devices are dominantly found in rigid form factors such as bracelets and pucks. An adhesive RFID sensor bandage (patch) is reported, which can be made completely intimate with human skin, a distinct advantage for chronological monitoring of biomarkers in sweat. In this demonstration, a commercial RFID chip is adapted with minimum components to allow potentiometric sensing of solutes in sweat, and surface temperature, as read by an Android™ smart-phone app with 96% accuracy at 50 mM Na^+ (*in-vitro* tests). All circuitry is solder-reflow integrated on a standard Cu/polyimide flexible-electronic layer including an antenna, but while also allowing electroplating for simple integration of exotic metals for sensing electrodes. Optional paper microfluidics wick sweat from a sweat porous adhesive allowing flow to the sensor, or the sensor can be directly contacted to the skin. The wearability of the patch has been demonstrated for up to 7 days, and includes a protective textile which provides a feel and appearance similar to a standard Band-Aid®. Applications include hydration monitoring, but the basic capability is extendable to other mM ionic solutes in sweat (Cl^-, K^+, Mg^{2+}, NH_4^+, Zn^{2+}). The design and fabrication of the patch is provided in full detail, as the basic components could be useful in the design of other wearable sensors.**

***Index Terms*—flexible electronics, RFID, biosensor**

Reprinted from IEEE

Manuscript received June 18, 2014; revised September 10, 2014; accepted November 6, 2014. This work was supported in part by the U.S. Air Force-Air Force Research Labs and the National Science Foundation (EECS EAGER, #1347725).

D. P. Rose, M. Ratterman, & D. K. Griffin are with the Department of Electrical Engineering & Computing Systems at the University of Cincinnati, Cincinnati, OH 45221 USA (email: rosedp@mail.uc.edu; ratterme@mail.uc.edu; griffid6@mail.uc.edu).

L. Hou was with the University of Cincinnati, Cincinnati, OH 45221 USA. She is now with Intel Corporation, Hillsboro, OR 97124 USA (e-mail: linlin.hou@gmail.com).

J. Heikenfeld & I. Papautsky are with the Department of Electrical Engineering & Computing Systems at the University of Cincinnati, Cincinnati, OH 45221 USA (email: heikenjc@ucmail.uc.edu; papauti@ucmail.uc.edu).

J. A. Hagen, N. Kelley-Loughnane, & R. Naik are with the Air Force Research Labs, Dayton OH 45233 USA (email: joshua.hagen.1@us.af.mil, nancy.kelley-loughnane@us.af.mil, rajesh.naik@us.af.mil, respectively).

Digital Object Identifier 10.1109/TBME.2014.xxxxxx

Android is a trademark of Google Inc.; Nike+ is a trademark of Nike Inc.; FitBit is a trademark of FitBit Inc.

Copyright (c) 2013 IEEE. Personal use of this material is permitted. However, permission to use this material for any other purposes must be obtained from the IEEE by sending an email to pubs-permissions@ieee.org.

I. INTRODUCTION

SWEAT is one of few examples of non-invasively accessed biofluids, with potential advantages in measurement of inflammatory biomarkers compared to saliva [1] and potentially superior time-resolved (chronological) readings of biomarker concentrations compared to saliva and urine. Sweat access can be locally stimulated using FDA-approved iontophoresis (Wescor Macroduct), and recent tattoo-like sweat-sensing demonstrations further include measurement of lactate, ammonium, and sodium [2-4]. A particularly attractive application could be hydration and heat-stress monitoring through electrolyte balance (e.g., Na^+, K^+) for athletes, military personnel, first-responders, and others working in extreme-conditions. Electrolyte sensing is of further value, because the high salinity of sweat can confound other biomarker readings, hence electrolyte concentrations need to be base-lined. Realizing such wearable sensors could be achieved several ways, including wearable textiles[5], tattoos[3, 6, 7], and form-factors such as those seen commercially in digital bracelet products such as Nike+™ and Fitbit™. However, a complete wireless sensor with wearability comparable to a simple Band-Aid® that is low cost, robust, communicates with smart phones and exhibits a design which automatically lends itself to maximum time-resolved readings of sweat has not yet been demonstrated.

A wearable, medical-grade adhesive RFID enabled sensor patch is reported, which is conformal to the shape of the human body, and therefore minimizes dead volumes of sweat which would otherwise limit chronological measurements. Adaptation of a commercial RFID chip is achieved with minimum components to allow potentiometric sensing of electrolytes in sweat as well as skin surface temperature, and could be of use for hydration and heat-stress monitoring. The patch is battery-free, powered and read wirelessly by an Android smart phone and custom-app. From *in-vitro* solution to smart-phone readout, a dynamic range of 235 mV to 255 mV is achieved with 20 mM to 70 mM range and 96% accuracy in the detection of Na^+ concentration. All circuitry is solder-reflow integrated on a standard Cu/polyimide flexible-electronic layer including conventional components such as an antenna, but also allowing electroplating for simple integration of exotic metals for ion-selective sensing electrodes. The sensing electrodes can be folded over to be in direct contact

0018-9294 (c) 2013 IEEE. Personal use is permitted, but republication/redistribution requires IEEE permission. See http://www.ieee.org/publications_standards/publications/rights/index.html for more information.

This article has been accepted for publication in a future issue of this journal, but has not been fully edited. Content may change prior to final publication. Citation information: DOI 10.1109/TBME.2014.2369991, IEEE Transactions on Biomedical Engineering

with skin, or paper microfluidics can be used to wick sweat from the skin and to the sensors. The wearability of the patch has been shown up to 7 days, and includes a protective textile which provides a feel and appearance similar to a standard Band-Aid or transdermal patch. This work outlines a complete integration of the key materials, electronics, microfluidics, and ergonomics, required for a wearable sweat sensing patch, paving the way for future wearable sweat sensor development and *in-vivo* testing. Applications include hydration monitoring, but the basic capability is extendable to other mM solutes in sweat (Cl^-, K^+, Mg^{2+}, NH_4^+, Zn^{2+}). Full details of the design and fabrication of the patch are reported, as the basic components could be of use to other wearable sensor applications. A preliminary version of this work has been initially accepted as proceedings of IEEE EMBC'14.

II. Top-Level Design Considerations

A. Patch Size

Two patch sizes were chosen and demonstrated. The smaller size (~25 x 60 mm) of a typical Band-Aid was used for high user acceptance. A larger 70 x 40 mm patch was also demonstrated, a size similar to bandage that might be placed over a knee. To allow a maximally thin form factor, potentially longer shelf-life, and low cost, the patch was designed for battery-free RFID (radio-frequency ID, inductively powered) operation. RFID requires ~10-20 loops of a coiled antenna to power the electronics (depending on patch size). The resulting area interior to the coil is more than sufficient for placement of the necessary electronics and the sensor electrodes (as visible in Fig. 1). The larger of the two patch antenna sizes was found to be more resilient to variations in antenna fabrication (antenna resonance), and provides greater reliability in communication. Patches even smaller than those demonstrated here are possible (see online supplemental file on antenna design).

B. Communication

For communication, most modern smartphones have, or will have, the capability to establish wireless connections and transfer data via a near-field communication RFID protocol. The patch is designed to operate on the standard ISO-15693 as a vicinity device. This provides the desired versatility in communication through stand-alone RFID readers as well as customizable applications ('apps') for RFID-enabled Android smartphones. The ubiquity of smartphones provides an easily accessible computing platform with increased memory/storage capabilities, thereby eliminating the need for on-patch data logging and the additional circuitry, cost, size it would require.

C. Flexible & Wearable

Flexibility is of paramount concern in wearable electronics, along with strength and durability. The flexible printed circuit board (PCB) is built from Dupont Pyralux – a combination of flexible, conformal polyimide and a thin copper foil. The high heat tolerance of the polyimide allows for electronics to be attached by solder reflow. Furthermore, solder reflow allows surface-mount packaging which eliminates need for through-holes that would result in protrusions that would cause discomfort when the patch is worn. For packaging and skin adhesion, a survey of numerous medical-grade textiles from 3M™ was conducted to determine which materials would provide maximum adhesion to the wearer's skin and high durability to protect the patch itself. Double sided medical adhesive tape was used below the patch, whereas above the patch, a medical textile covering was added to protect the patch and improve visual aesthetics (all shown in Fig. 1).

(a) phone and smallest communicating patch



(b) patch photgraphs

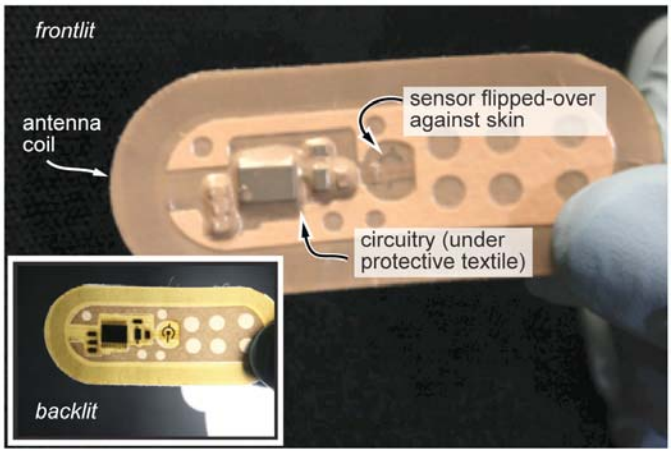


Fig. 1 Device photographs (a) shown on body and (b) to illustrate electronic and sensor features.

D. Basic Electronics and Programming Functionality

The system level block diagram shown in Fig. 2 illustrates the system level layout of the patch functionality beginning and ending with communication between the reader device and the patch. The reader device initiates the communication and requests identification from the patch. The patch responds by load modulating the inductive coupling between itself and the RFID reader. Custom commands for programming include reading, writing to memory registers, sensor configuration, power management, and other functionalities not required for this present work.

The primary chip in the patch is a small Melexis

0018-9294 (c) 2013 IEEE. Personal use is permitted, but republication/redistribution requires IEEE permission. See http://www.ieee.org/publications_standards/publications/rights/index.html for more information.

This article has been accepted for publication in a future issue of this journal, but has not been fully edited. Content may change prior to final publication. Citation information: DOI 10.1109/TBME.2014.2369991, IEEE Transactions on Biomedical Engineering

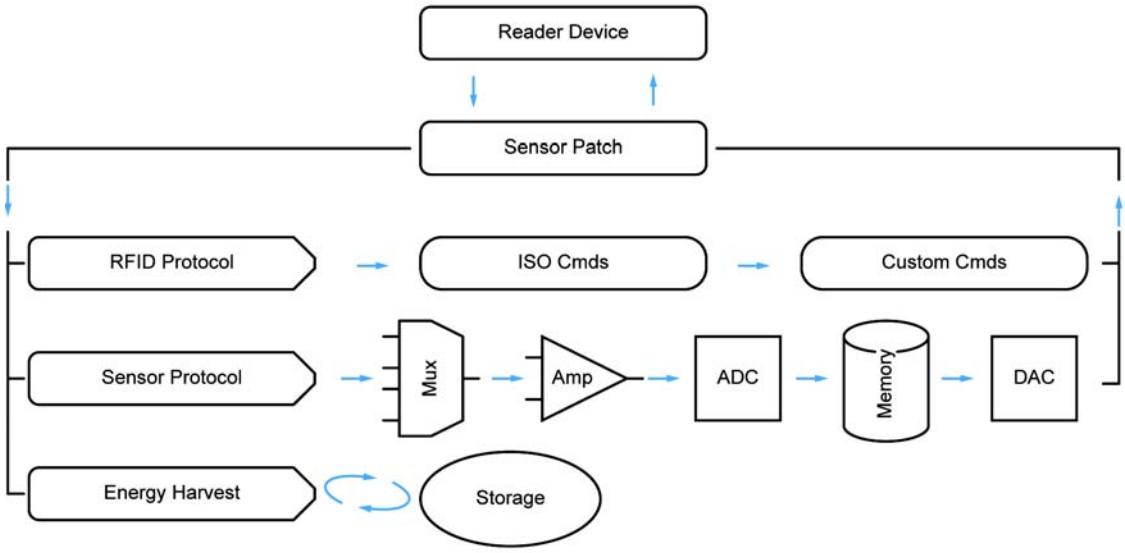


Fig. 2 System level block diagram

MLX90129 RFID transponder chip which has both basic sensor and energy harvesting capabilities. The chip functionality is explained in detail here, because its use could be adapted to a large variety of other sensor applications. A significant amount of programming development was required to enable a smart phone to turn the RFID chip into an electrolyte sensor. With further reference to Fig. 2, the sensor protocol manages tasks assigned to the MLX90129's sensor pins such as input connections, voltage output to external sensors, and enabling the internal temperature sensor. Four input pins provide differential measurement of potential from externally connected sensors (e.g. ion selective electrodes in this work). Two internal connections can enable the output of the onboard temperature sensor to be used as input into the multiplexer. Configuration of the multiplexer determines which inputs are passed to the first programmable gain amplifier (PGA). If enabled, the digital to analog converter (DAC) can set the offset used in the optional second PGA. The 12-bit ADC converts the amplified sensor outputs for storage in digital memory until the DAC converts the digital measurements for analog transmission to the reader.

Battery-free operation is achieved by utilizing energy harvesting circuitry of the MLX90129 which utilizes the induced current of the incoming electromagnetic waves from the reader to power the entire patch. To facilitate the power demands of the various IC processes, an external capacitor and diode are added for charge storage. The siphoned charge is used to complete low power processes during brief interruptions or absences of induced current from the reader device. Battery independence improves the potential shelf-life of such patches.

III. Detailed Fabrication - Electronics

1) Flexible Circuit Board

Fabrication begins at the flexible electronic circuit board (Fig. 3) with a sheet of Dupont Pyralux AC (18 µm thick Cu foil clad to 12 µm Kapton). A 127 x 101.6 mm substrate is first cut from the bulk Pyralux roll. As the integrity of the copper surface is imperative, great care must be taken to minimize creases, dimples, and other surface imperfections. Therefore even during substrate cleaning, the substrate is supported by a rigid silicon carrier. The substrate is cleaned of any residual oils, fingerprints or other contaminants by submerging it in a 120 °C alkaline solution of Na_2CO_3 (9.2 wt%), 50% NaOH (4.6 wt%), Triton X-100 (surfactant, 0.2 wt%) and reverse osmosis (RO) H_2O (86.0 wt%). The sample is left in the solution for a minimum of 10 min and agitated approximately every 2 to 3 min, and then rinsed thoroughly in RO water. Once rinsed and dried in N_2, the substrate is then placed in a bath of reagent grade H_2SO_4 (10 wt%) for 5 min to remove the manufacturer's anti-tarnish coating and prepare the sample for lithography. As before, the copper is thoroughly rinsed in RO water and dried in N_2.

To pattern the Cu, Shipley S1818 positive tone, liquid photoresist is coated on the copper substrate using traditional spin-coat techniques. For the spin-coat process, the substrate is bonded to 6 inch silicon wafer using a droplet of water, smoothed via a plastic blade for uniform pressure, and held in place by capillary adhesion.

The S1818 resist is spun first at 500 rpm for 30 s and then at 2500 rpm for 60 s to achieve a target thickness between 2 to 2.5 µm (a thicker resist is more durable during the etching process). The substrate and the Si carrier are then "soft" baked in an oven set at 100 °C for 150 s. The carrier and copper substrate are removed from the oven and allowed to cool briefly before masking and 365 nm UV exposure at 150 mJ/cm^2 for 25 s. Developing of the resist is accomplished by placing the substrate and carrier for 45 s into an agitated ~21°C bath of Microposit 351 photoresist developer diluted with RO to a 1:4 (v/v) ratio. This solution is slightly more aggressive than the more common 1:5 ratio, however, the higher concentration developer performs better at removing the exposed photoresist from the non-uniform features of the copper surface and therefore results in a more consistent etch

Reprinted from IEEE

0018-9294 (c) 2013 IEEE. Personal use is permitted, but republication/redistribution requires IEEE permission. See http://www.ieee.org/publications_standards/publications/rights/index.html for more information.

This article has been accepted for publication in a future issue of this journal, but has not been fully edited. Content may change prior to final publication. Citation information: DOI 10.1109/TBME.2014.2369991, IEEE Transactions on Biomedical Engineering

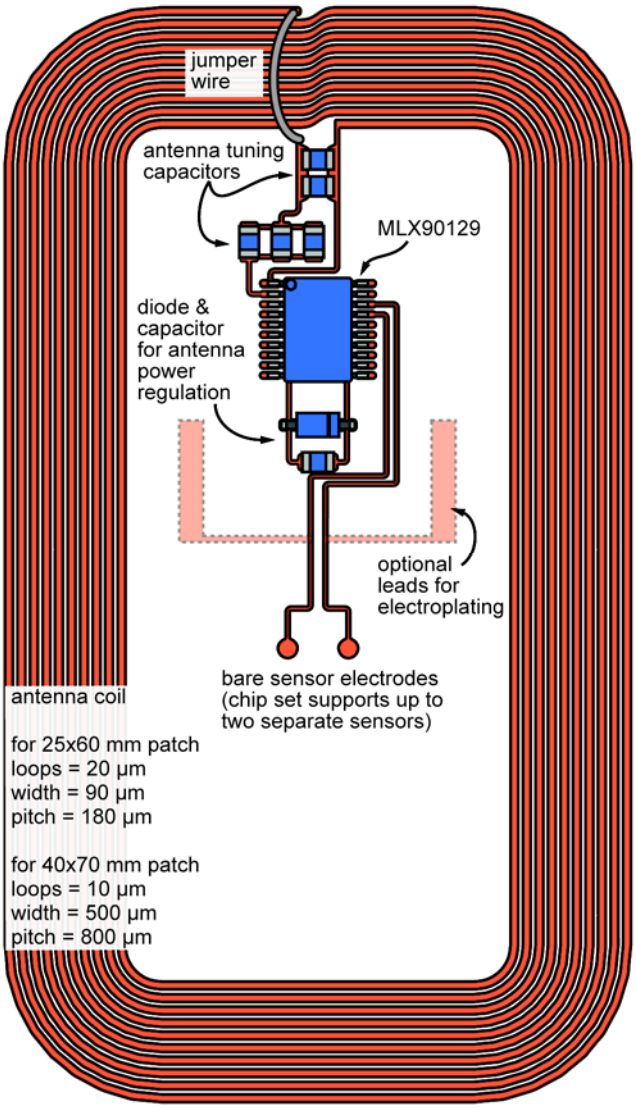


Fig. 3 Circuit layer layout detailing antenna coil geometry and electronics placement.

time and cleaner etch results. During development of the photoresist the Si carrier detaches from the substrate so that great care must be taken during rinsing and drying of the substrate after development.

Etching of the exposed copper is accomplished by an air bubble agitated acid bath in which the substrate is secured with PTFE screws to a plastic acrylic carrier and submerged vertically positioned for 30 s. The acid bath is comprised of a diluted reagent HCl solution (30 wt%) and diluted solution of 30% H_2O_2 (3 wt%) combined at a ratio of 2:1 by volume. After etching is complete, the substrate and carrier are thoroughly rinsed in a spray of RO water for a minimum of 60 s and dried using compressed N_2. The substrate is then carefully removed from the acrylic carrier and placed on the Si wafer for photoresist stripping. The S1818 photoresist is removed by submerging the sample and Si carrier in a bath of full concentration Shipley 351 photoresist developer. The bath is manually agitated once every 30 s for 5 min or until all the photoresist has been removed from the Cu surface. A final rinse and dry step is performed and electrical continuity tests

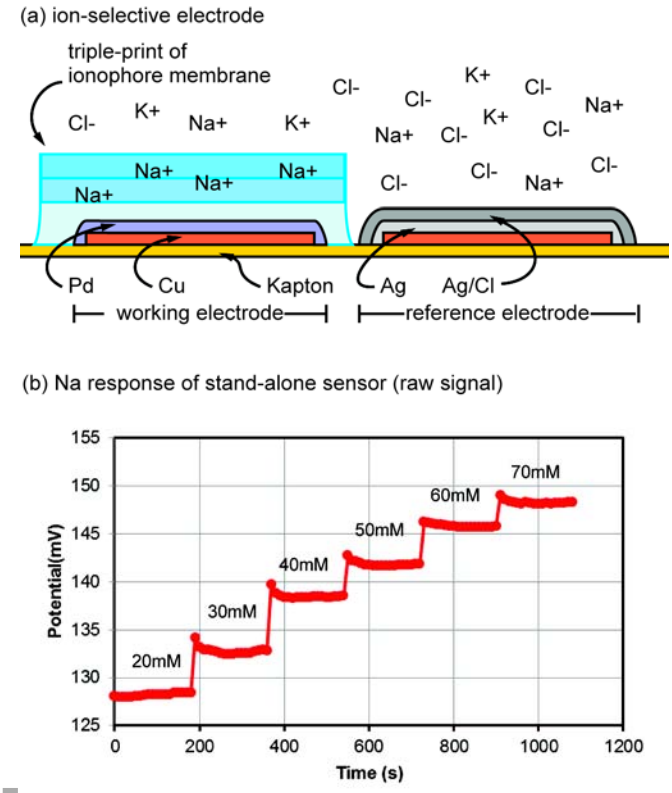


Fig. 4 (a) Ion-selective electrode fabrication and (b) raw sensor potential for several concentrations of Na^+ in water (measured independent of the patch and its circuitry).

are used to verify the integrity of the antenna coil traces, sensor electrode traces and other critical connections.

2) Plating of Sensor Electrodes

The sensors are fabricated in two steps, one before and one after the electronic chip attachment. In the first step, the working and reference electrodes of the sensor (Fig. 4a) are fabricated by electrodeposition of Pd and Ag on the previously-defined bare copper electrodes (Fig. 3). This is accomplished using plating solutions from Technic, Inc. and deposition at ~5mA/cm^2 anodic current for 90 s with a Pt wire auxiliary electrode to sustain the current. The reference electrode fabrication is then completed by chloridization of the Ag layer in 1 M KCl with a 3 mA/cm^2 anodic current for 30 s to form the reference.

3) Chip Attachment

Before chip attachment, the inductance of the antenna coil is measured to determine the needed values of the tuning capacitors shown in Fig. 4. An alloy of Sn/Ag (96.5/3.5%) no-clean solder paste (Superior Flux & Mfg. Co. P/N: 3033-85) is applied to each pad using an air-metered syringe dispenser, or higher volume fabrication by stencil printing. The chips are then placed, and also an insulated jumper wire (Fig. 3) is placed to connect to the outer loop of the coil. The flex circuit board is then placed in a programmable, convection reflow oven that applies a heating profile according to the solder supplier specification. The reflow oven is connected to a pressurized N_2 gas supply, which is used to purge the sample chamber and prevent oxidation of the Cu surfaces.

4) Hermetic Sealing of Electronics

In applications where fluid contact could occur, such as

0018-9294 (c) 2013 IEEE. Personal use is permitted, but republication/redistribution requires IEEE permission. See http://www.ieee.org/publications_standards/publications/rights/index.html for more information.

This article has been accepted for publication in a future issue of this journal, but has not been fully edited. Content may change prior to final publication. Citation information: DOI 10.1109/TBME.2014.2369991, IEEE Transactions on Biomedical Engineering

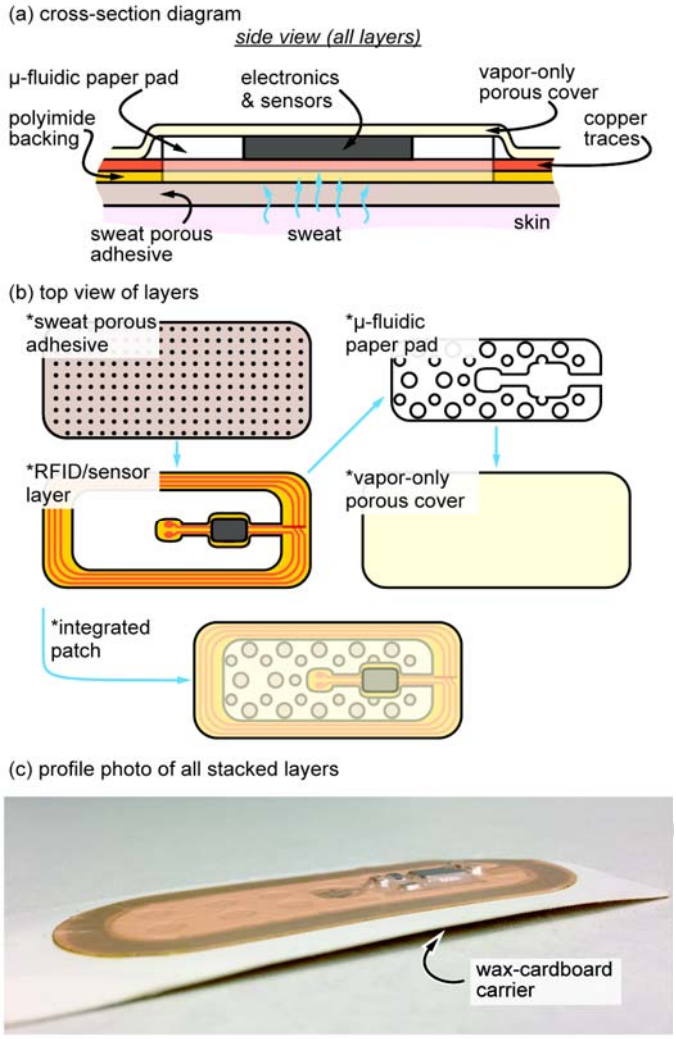


Fig. 5 Device layer integration: (a) cross-section, (b) top view and (c) profile of completed device.

sweat sensing, the electronics must be hermetically sealed. This is easily achieved by masking the sensor electrodes with Kapton Tape (silicone adhesive), and conformally coating the flexible circuit and electronics with 10s of μm of Parylene C polymer dielectric using a Specialty Coating Systems 2010 Lab Coater. Ideally this is performed before sensor functionalization, to ensure the Kapton masking tape does not damage or contaminate the final sensor surfaces.

5) Sensor Functionalization

Onto the plated sensor electrodes, the polymer ionophore (ion-selective) membrane is cast (Fig. 4a). This is performed after chip attachment because the high temperature required for chip solder reflow would damage the polymer membranes. The membrane solution was cast carefully over the working electrode using a modified screen printing process. The membrane was made from a cocktail of sodium ionophore X, bis(2-ethylhexyl) sebacate (DOS), potassium tetrakis (p-chlorophenyl)borate (KTpC1PB), PVC, and cyclohexanone, then manually mixed together until the PVC was fully dissolved. The cast membranes were left to air dry for 8 hours, then coated 2 more times to ensure adequate coverage of the electrodes and to passivate any pores in the membrane that could cause shorting to the electrodes[8, 9].

The Na^+ sensor is based on a traditional ion selective electrode (ISE), but which has been miniaturized in this work. The Na^+ selective ionophore membrane establishes a difference in potential across the electrode-ionophore barrier corresponding to the Na^+ concentration, enabling a simple potentiometric measurement. The level of Na^+ in the solution is given by the Nernst equation: $E = E_0 + S\ log(X)$, where E is the measured electrode potential, E_0 is the reference electrode potential, S is the sensitivity, and X is the concentration of Na^+ ions in solution. Although in this work only sensing of Na^+ is demonstrated, sensing of other ions in sweat (Cl^-, K^+, Mg^{2+}, NH_4^+, Zn^{2+}) could be demonstrated using appropriate commercially available ionophores from Sigma Aldrich.

6) Substrate Cutting

The patch is a wearable sensor, and therefore all unused portions of gas/liquid impermeable polyimide substrate film should be removed to provide skin access, and to improve breathability of the final patch. Cutting is performed using a Universal Laser Systems VLS3.50 CO_2 laser cutter. The areas that are trimmed include area outside the antenna coil, and the unused interior portion, including the electroplating leads (Fig. 3).

IV. Integration – Electronics, Textiles, Skin Adhesives, and Microfluidics

As shown in Fig. 5, the final device integration involves from the bottom up: skin adhesives, electronics, paper microfluidics, and a vapor porous top adhesive textile. All of these layers are laser cut. The bottom, double-sided adhesive layer is 3M™ Double Coated Polyester Tape (P/N: 1567) and cut to a 1 mm offset larger than the trimmed flex circuit layer. An array of circular pores is also laser cut in the bottom adhesive layer to facilitate sweat transmission to the sensor. The microfluidic paper layer is interior to the coil and surrounds the sensor electrodes and electronics. If the sensors are placed face-up (away from skin) then they are covered by the paper layer to bring sweat to the sensors. Extensive wearability studies have not been performed with the patch in this initial demonstration, and in the event that further breathability is needed by skin areas covered by flexible circuit substrate, then the paper-microfluidics layer can simply be integrated beneath the electronics layer to provide horizontal transport of vapor or fluid. The top protective layer is cut from 3M™ Tan Polyurethane Tape (P/N: 9834T) with single-sided adhesive. This layer is cut to the same outer dimensions as the bottom adhesive layer to provide an edge sealed seam for the completed patch.

Multi-layer integration is assisted by a custom alignment jig and vacuum forming/bonding table (1 atm. pressure). The bottom layer is affixed to a waxed paper carrier as shown in Fig. 5c. The flex circuit's sensor electrodes are then folded back and underneath its traces so that the active area of the sensor will be facing the skin. The flex circuit is placed on top of the bottom adhesive layer using the vacuum placement tool. Next, the microfluidic paper layer is placed between the coil and the rest of the circuitry. Finally, the top protective layer is

0018-9294 (c) 2013 IEEE. Personal use is permitted, but republication/redistribution requires IEEE permission. See http://www.ieee.org/publications_standards/publications/rights/index.html for more information.

This article has been accepted for publication in a future issue of this journal, but has not been fully edited. Content may change prior to final publication. Citation information: DOI 10.1109/TBME.2014.2369991, IEEE Transactions on Biomedical Engineering

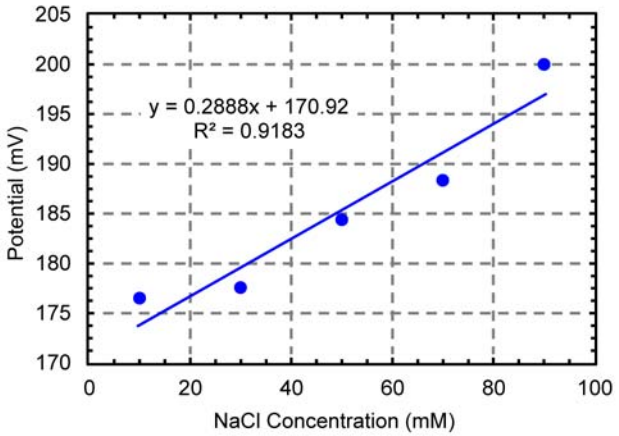


Fig. 6 Calibration curve showing sensitivity and linearity of patch to Na^+.

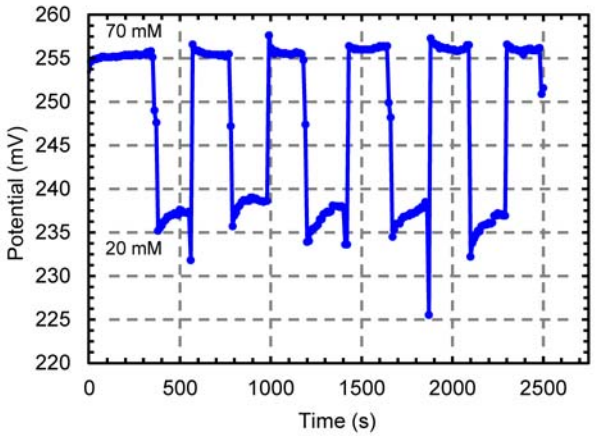


Fig. 7 Patch results for concentration variations from 20mM to 70mM NaCl.

aligned and placed by vacuuming; sealing the circuit and sensor within. A final communication test with the RFID reader is performed to verify operation, and the sweat sensor is ready for programming and use.

V. Experimental Testing And Results

A. Wearable Antenna Performance

The assembled RFID circuit was tested to ensure that the resonate frequency was near enough to the target frequency of 13.56 MHz that the device would communicate with the reader. A supplemental information document is provided with the online materials for this paper, detailing the finer details of the antenna design and tuning. To confirm antenna tuning, a vector network analyzer (VNA) was connected to an ISO standard calibration loop-probe, per ISO10373-7, to enable contactless measurement of the patch's frequency response. The VNA displays the loop-probe's reflection coefficient by measuring the S-parameter S11 as a function of frequency. A reduction in the reflection measured by the VNA correlates to an increase in transmission of the electromagnetic waves at a specific frequency, via absorption of the radiated energy by a tuned and coupled device. Successful tuning of the flexible RFID circuit was confirmed by a reduction of S11 by -2.9 dB at 13.56 MHz. With a reader RF power of ~ 0.5 W this tuning was also shown to be adequate to inductively power the electronics and enable RF communication. Patch communication was shown in wearable format, including arm placement which induces curvature on the entire patch.

B. Sensor and Electronics Performance

The patch and sensors were characterized *in-vitro* by pipetting of various NaCl concentration solutions onto the patch sensor. Fig. 4b illustrates sensor response as Na+ concentration increased from 20 mM to 70 mM. As expected, the sensor output increased with analyte concentration, exhibiting stable response at each concentration. At each concentration change, the sensor responded rapidly, with approx. 30 s response time. The standard curve, developed by measuring response of a stand-alone sensor in the 20-70 mM Na+ range against the commercial ISE from Denver Instruments (300741.1) exhibited a correlation coefficient of 0.99 (data not shown). These results clearly suggest that our sensor exhibits acceptable and predictable behavior for measurement of Na+. Fig. 6 shows the sensor calibration curve derived from testing 10 patches. As expected, the patch-integrated sensors exhibited a predictable linear response, with the correlation coefficient of 0.92. The range of 10mM to 90mM was chosen to ensure the detection range would be +/- 10 mM beyond physiologically relevant ranges for hydration monitoring [10, 11].

Sensitivity of the sensor in the integrated patch was 0.3 mV/mM, which was slightly lower than that the commercial sensor sensitivity of 0.5 mV/mM or approx. 25 mV/decade of Na+ concentration. While at first glance this suggests a sub-Nernstian behavior, we tested the stand-alone sensors, and obtained sensitivity of approximately 57 mV/decade of Na^+ in the 10-90 mM concentration range, indicating that the sensor exhibits Nernstian behavior. Similar results have been reported for Na^+ ISEs by others [8]. Thus, the apparent lower sensitivity of the patch-integrated sensors appears to be due to the limitations of the ADC on the RFID patch. The ADC reference voltage is set by the MLX90129's internal regulator, from which two values may be selected – normal reference of 3.1 V, or low-volt reference of 2.1 V. The minimum voltage of the chip's coil input is such that provided the chip powers on, the internal regulator will supply a stable reference to the ADC. However, since the sampling rate for the converter is slow (< 3Hz) for the desired accuracy the stabilization of the reference electrode on a specific voltage is impaired. The sampling rate used in Fig. 7 is approximately 3 Hz to achieve maximum resolution, while the maximum sampling rate of the device is approx. 435 Hz at the lowest conversion resolution.

Accuracy is an important characteristic for a sensor and measures how close the sensor is able to determine the true value of a given concentration. To measure accuracy of our RFID Na^+ sensor, we repeatedly measured 50mM of NaCl (n = 7), which was expected to yield 185mV based on the calibration curve. Response of our patch was measured to be 177 +/- 5 mV. These results show that at 50mM NaCl, our

Reprinted from IEEE

0018-9294 (c) 2013 IEEE. Personal use is permitted, but republication/redistribution requires IEEE permission. See http://www.ieee.org/publications_standards/publications/rights/index.html for more information.

This article has been accepted for publication in a future issue of this journal, but has not been fully edited. Content may change prior to final publication. Citation information: DOI 10.1109/TBME.2014.2369991, IEEE Transactions on Biomedical Engineering

patch sensor exhibits 96% accuracy. Precision is another important characteristic for a sensor and in essence it illustrates sensor variability. From the experimental data, the patch sensor exhibited 28% precision. However, precision is not provided for commercial ISEs, and the needed values will depend on application. Even simple measurement of trending (increase or decrease) of Na^+ itself is valuable, as Na^+ concentration predicts sweat rate as it increases by 10's of mM in concentration with increasing sweat rate. This patch therefore can be utilized even in its current form as an athletic exertion sensor, for example.

To further explore the potential for continuous monitoring in sweat, concentration of NaCl was varied repeatedly every 4 min from 20mM to 70mM over a period of 45 min. Na^+ concentration in sweat can vary from 20mM to 70mM depending on body hydration status [10, 11]. As shown in Fig. 7, the sensor exhibited good repeatability and stability during this measurement. The average high measurement was 255mV, which corresponds to 70 mM based on the calibration curve. The coefficient of variation across the 6 high concentration measurements was CV = 0.1%, indicating excellent repeatability. Similarly, the 5 low concentration measurements yielded approximately 237 mV, with CV = 0.8%. The response time at low concentration was slower, and is a function of the mass transport across the sensor ion-selective membrane. As with most electro-chemical sensors, stability of the reference electrode can be an issue and can lead to the inability to collect stable data. Our sensor exhibited only a slight drift (+/-3mV/5mM), however by increasing sampling frequency and averaging the values we were able to compensate for this difference. Future work will involve further stabilizing of the Ag/AgCl reference electrode to increase stability of the measured values. Collectively, these results suggest that the developed sensor is suitable for sweat electrolyte monitoring.

VI. Discussion And Conclusions

The primary objective of this work was to demonstrate the complete integration of the components and functionality needed for a low-cost and highly self-contained sweat sensor. A collection of key performance data and cost-estimates is provided in Table 1. The most expensive single component, is the Melexis RFID chip, at <$2 in volume purchasing right now. The remainder of the components and fabrication procedures for the patch are rather simple and implementable on most flexible and printed electronics manufacturing lines. Therefore the basic patch presented here could be speculated at this time to meet the economic considerations of a disposable commercial product.

The key question in the applied value for this work is in terms of performance. The performance for the existing patch is shown to be adequate and accurate for basic sensing at physiological relevant levels in sweat, and would increase in performance with higher sampling frequency, improved power management, sensor signal conditioning and conversion efficiency of the analog sensor inputs. Establishing the basic functionality shown in this paper is important, because numerous other ionophores and ion selective electrodes, or measurements, could be integrated with the patch, allowing a broader range of applications for the sensor. The current sensor measures Na^+, and using the second sensor port to measure K^+ would be intended to explore ratios of electrolytes in relation to hydration (hence the term, 'electrolyte balance'). Other ions of interest include Cl^-, Mg^{2+}, NH_4^+, which expand the physiological readings that could be made from human sweat. Devices such as this, and others [4, 12-15], could mark the beginning of an entirely new way of monitoring human physiology and performance. Wearable and wireless devices that are unobtrusive to the user fill a critical gap in the technology needed to collect real time data on the health status of our most precious assets – people.

TABLE I
Preliminary Patch Specifications

Specification	Value
Size	61 x 25 x 1.2 mm (min) 72 x 42 x 2 mm (typical)
Wearability	Adheres for up to 7 days.
Sensors	2 (max)
Expanded Capability	Available battery and microcontroller connect.
Low-volume BOM	$6.00 / patch – Volumes of 1-10.
Max Data	3.5 kbits
Reader Power	0.5 Watts (typical)
Frequency	13.56 MHz
Na^+ Range	10 mM – 90 mM
Na^+ Accuracy	±5 mM (96%) at 50 mM
Na^+ Precision	28%
Temperature Range	-40 °C to +105 °C (full range)

Reprinted from IEEE

VII. Additional Acknowledgements

The authors would like to thank Theresa Gerten, Senior Biologist at 3M™, for guidance and sampling of skin adhesives, the Air Force Research Laboratory (711th Human Performance Wing and Materials and Manufacturing Directorate) and the National Science Foundation EECS Division for financial support.

References

[1] G. Cizza, A. H. Marques, F. Eskandari, I. C. Christie, S. Torvik, M. N. Silverman, T. M. Phillips, and E. M. Sternberg, "Elevated neuroimmune biomarkers in sweat patches and plasma of premenopausal women with major depressive disorder in remission: the POWER study," *Biological psychiatry,* vol. 64, no. 10, pp. 907, 2008.

[2] M. J. Buono, C. S. White, and K. P. Connolly, "Cholinergic sensitivity of the eccrine sweat gland in trained and untrained men," *Journal of dermatological science,* vol. 4, no. 1, pp. 33-37, 1992.

[3] T. Guinovart, A. J. Bandodkar, J. R. Windmiller, F. J. Andrade, and J. Wang, "A potentiometric tattoo sensor for monitoring ammonium in sweat," *Analyst,* vol. 138, no. 22, pp. 7031-7038, 2013.

[4] A. J. Bandodkar, D. Molinnus, O. Mirza, T. Guinovart, J. R. Windmiller, G. Valdés-Ramírez, F. J. Andrade, M. J. Schöning, and J. Wang, "Epidermal tattoo potentiometric sodium sensors with wireless signal transduction for continuous non-invasive sweat monitoring," *Biosensors and Bioelectronics,* vol. 54, pp. 603-609, 2014.

[5] S. Coyle, K. T. Lau, N. Moyna, D. O'Gorman, D. Diamond, F. Di Francesco, D. Costanzo, P. Salvo, M. G. Trivella, D. E. De Rossi, N. Taccini, R. Paradiso, J. A. Porchet, A. Ridolfi, J. Luprano, C. Chuzel, T.

0018-9294 (c) 2013 IEEE. Personal use is permitted, but republication/redistribution requires IEEE permission. See http://www.ieee.org/publications_standards/publications/rights/index.html for more information.

This article has been accepted for publication in a future issue of this journal, but has not been fully edited. Content may change prior to final publication. Citation information: DOI 10.1109/TBME.2014.2369991, IEEE Transactions on Biomedical Engineering

Lanier, F. Revol-Cavalier, S. Schoumacker, V. Mourier, I. Chartier, R. Convert, H. De-Moncuit, and C. Bini, "BIOTEX—Biosensing Textiles for Personalised Healthcare Management," *Information Technology in Biomedicine, IEEE Transactions on,* vol. 14, no. 2, pp. 364-370, 2010.

[6] A. J. Bandodkar, V. W. S. Hung, W. Jia, G. Valdés-Ramírez, J. R. Windmiller, A. G. Martinez, J. Ramírez, G. Chan, K. Kerman, and J. Wang, "Tattoo-based potentiometric ion-selective sensors for epidermal pH monitoring," *Analyst,* vol. 138, no. 1, pp. 123-128, 2013.

[7] W. Jia, A. J. Bandodkar, G. Valdes-Ramirez, J. R. Windmiller, Z. Yang, J. Ramirez, G. Chan, and J. Wang, "Electrochemical Tattoo Biosensors for Real-Time Noninvasive Lactate Monitoring in Human Perspiration," *Analytical chemistry,* vol. 85, no. 14, pp. 6553-6560, 2013.

[8] S. Walsh, D. Diamond, J. McLaughlin, E. McAdams, D. Woolfson, D. Jones, and M. Bonner, "Solid-state sodium-selective sensors based on screen-printed Ag/AgCl reference electrodes," *Electroanalysis,* vol. 9, no. 17, pp. 1318-1324, 1997.

[9] F. Phillips, K. Kaczor, N. Gandhi, B. D. Pendley, R. K. Danish, M. R. Neuman, B. Toth, V. Horvath, and E. Lindner, "Measurement of sodium ion concentration in undiluted urine with cation-selective polymeric membrane electrodes after the removal of interfering compounds," *Talanta,* vol. 74, no. 2, pp. 255-264, 2007.

[10] M. J. Patterson, S. D. R. Galloway, and M. A. Nimmo, "Variations in regional sweat composition in normal human males," *Experimental Physiology,* vol. 85, no. 6, pp. 869-875, 2000.

[11] T. Verde, R. J. Shephard, P. Corey, and R. Moore, "Sweat composition in exercise and in heat," *Journal of Applied Physiology,* vol. 53, no. 6, pp. 1540-1545, 1982.

[12] J. Weber, A. Kumar, A. Kumar, and S. Bhansali, "Novel lactate and pH biosensor for skin and sweat analysis based on single walled carbon nanotubes," *Sensors and Actuators B: Chemical,* vol. 117, no. 1, pp. 308-313, 2006.

[13] B. Schazmann, D. Morris, C. Slater, S. Beirne, C. Fay, R. Reuveny, N. Moyna, and D. Diamond, "A wearable electrochemical sensor for the real-time measurement of sweat sodium concentration," *Analytical Methods,* vol. 2, no. 4, pp. 342-348, 2010.

[14] M. Strauss, C. Reynolds, S. Hughes, K. Park, G. McDarby, and R. W. Picard, "The handwave bluetooth skin conductance sensor," *Affective computing and intelligent interaction*, pp. 699-706: Springer, 2005.

[15] M.-Z. Poh, N. C. Swenson, and R. W. Picard, "A wearable sensor for unobtrusive, long-term assessment of electrodermal activity," *Biomedical Engineering, IEEE Transactions on,* vol. 57, no. 5, pp. 1243-1252, 2010.



Daniel P. Rose (GS'14) is a native of Cincinnati, Ohio. Daniel is a graduate of LaSalle High School ('99) and received his bachelor of science in physics from the University of Cincinnati in 2012.

From 2005 to 2008 he served as a rifleman in United States Marine Corps as part of Company E, 2[d] Battalion, 6[th] Marine Regiment, 2[d] Marine Division, including a deployment to Fallujah, Iraq in 2007. During the summers of 2009 and 2010 he was an undergraduate Research Assistant for the Nano-Materials Physics Group, headed by Profs. Howard Jackson and Leigh Smith at the University of Cincinnati, and was a Teaching Assistant for undergraduate physics laboratory courses during the academic years. In 2011 and 2012, he was a Research Intern with electrofluidic display developers Gamma Dynamics. He is currently a Graduate Research Assistant at the University of Cincinnati as a member of Prof. Jason Heikenfeld's Novel Devices Lab.



Michael E. Ratterman is originally from Indianapolis, Indiana and received his bachelor of science in EE from the University of Cincinnati in 2009. During this time Michael received the Best of EE award as a member of his Senior Project Development Team at the Cincinnati Tech Expo for their project "Smart Heart".

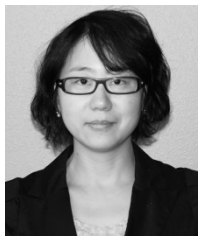
Previously he served aboard the USS Providence (SSN-719) as an Electrician's Mate (Nuclear) where he was qualified in electric plant operation as well as submarine casualty response tactics. He is currently a Graduate Research Assistant at the University of Cincinnati as a member of Prof. Ian Papautsky's Bio Micro Systems Lab. His research interests include optical-gas sensing, embedded firmware design, and electro-chemistry.



Daniel K. Griffin is an undergraduate researcher currently pursuing a bachelor's degree in computer engineering at the University of Cincinnati.

He has worked on numerous projects with the Novel Device Laboratory at the University of Cincinnati and 711th Human Performance Wing at Wright Patterson Air Force Base Research Laboratories.

Mr. Griffin has received numerous awards during his college career, including the national Goldwater scholarship for excellence in the sciences, engineering, and mathematics. Other awards include the University of Cincinnati EECS Mantei Mae award for his freshman, sophomore, and pre-junior years.



Linlin Hou received a B.S. in Measure Control Technology & Instruments and M.S. in Optical Engineering at the University of Shanghai for Science & Technology in 2002 and 2006, and Ph.D. in Electrical Engineering from the University of Cincinnati in 2012.

Dr. Hou previously worked in the Novel Devices Laboratory led by Dr. Heikenfeld at the University of Cincinnati from 2012 to 2013 as a postdoctoral researcher. Dr. Hou is now working at Intel as a Process TD Engineer in Portland, OR.

Reprinted from IEEE

0018-9294 (c) 2013 IEEE. Personal use is permitted, but republication/redistribution requires IEEE permission. See http://www.ieee.org/publications_standards/publications/rights/index.html for more information.

This article has been accepted for publication in a future issue of this journal, but has not been fully edited. Content may change prior to final publication. Citation information: DOI 10.1109/TBME.2014.2369991, IEEE Transactions on Biomedical Engineering



Nancy Kelley-Loughnane received a BS in chemistry from the University of New Hampshire, a PhD in biochemistry from Boston College.

She served as postdoctoral fellow at Cincinnati Children's Hospital Medical Center in 2001. Currently, she is an Air Force research biochemist and the Technical Advisor for Human Signatures Branch within the 711 Human Performance Wing at the Air Force Research Laboratory at Wright-Patterson Air Force Base, OH.

Dr. Kelley-Loughnane's research integrates her expertise in the fields of synthetic biology, protein chemistry, genomics, bioinformatics, and molecular biology. She leads a multidisciplinary research team focused on enhancing human performance through the identification of key biological signatures and the development of sensors to detect critical and operationally relevant physical and cognitive performance indicators.



Rajesh R. Naik received a B.S. in Microbiology from the University of Bombay and Ph.D. in Biological Sciences from Carnegie Mellon University. He is the research team leader for biological materials research in the Functional Materials Division, Materials and Manufacturing Directorate, Air Force Research Laboratory, Wright-Patterson Air Force Base, Ohio. His group conducts research in the area of bionanotechnology and biomimetics with focus on biosensing and bioelectronics. He is a Fellow of the Air Force Research Laboratory, Royal Society of Chemistry and SPIE.



Joshua A. Hagen received a B.S. in Chemical Engineering and M.S. and Ph.D. degrees in Materials Engineering from the University of Cincinnati in 2000, 2004 and 2006, respectively. Dr. Hagen currently works for the Air Force Research Labs in the 711th Human Performance Wing at Wright Patterson Air Force Base.

He leads a research group in Human Centric Sensor Systems with a focus on total physiological monitoring for applications ranging from personalized performance to the medical mission space.



Ian Papautsky (S'96-A'00-M'03-SM'08) received BS in biomedical engineering from Boston University in 1995 and PhD in bioengineering from the University of Utah in 1999. He is currently a Professor in the Dept. of Electrical Engineering and Computing Systems at the University of Cincinnati and Director of the BioMicro Systems Laboratory.

Dr. Papautsky is the Director of Ohio Center for Microfluidics Innovation (OCMI) and Co-Director of the newly formed NSF Center for Advanced Design & Manufacturing of Integrated Microfluidics. His current research interests focus on developing disposable microfluidic lab-on-a-chip systems and bio/chemical sensors for point-of-care applications.



Jason C. Heikenfeld (S'98-M'01-SM'06) received the B.S. and Ph.D. degrees from the University of Cincinnati in 1998 and 2001, respectively. After co-founding his 1st startup company, he returned to the University of Cincinnati as a Professor in the Dept. of Electrical Engineering and Computing Systems.

Dr. Heikenfeld's university laboratory, The Novel Devices Laboratory www.ece.uc.edu/devices, is currently engaged in electrofluidic device research for biosensors, beam steering, lab-on-chip, displays, and electronic paper. He has been awarded NSF CAREER and is both an AFOSR and Sigma Xi Young Investigator. Dr. Heikenfeld is a Senior member of the Institute for Electrical and Electronics Engineers, a Senior member of the Society for Information Display, and a member of SPIE, a member of ASEE, Fellow of the National Academy of Inventors, and a Fellow of the Univ. Cincinnati Academy For Teaching and Learning. In addition to his scholarly work, Dr. Heikenfeld launched two additional companies which are now active, he is an award winning educator, and has lead the creation of programs and coursework at the University of Cincinnati that foster innovation, entrepreneurship, and an understanding of the profound change that technology can have on society.

Reprinted from IEEE

0018-9294 (c) 2013 IEEE. Personal use is permitted, but republication/redistribution requires IEEE permission. See http://www.ieee.org/publications_standards/publications/rights/index.html for more information.